J|A|C|S
ARTICLES

Published on Web 05/14/2010

Molecular Order in a Chromonic Liquid Crystal: A Molecular Simulation Study of the Anionic Azo Dye Sunset Yellow

Fatima Chami and Mark R. Wilson*

Department of Chemistry, Durham University Science Laboratories, South Road, Durham DH1 3LE, U.K.

Received March 24, 2010; E-mail: mark.wilson@durham.ac.uk

Abstract: We have carried out a detailed atomic simulation study of molecular order within a chromonic liquid crystalline material (sunset yellow) in aqueous solution. Self-assembly occurs in dilute solutions to form stacked aggregates, which show a preference for head-to-tail stacking and antiparallel dipole order. This feature is independent of solution concentration and aggregate size. Stacks are found to be dynamic entities in which rotational transitions (flips) can occur between antiparallel and parallel configurations. At a concentration matching the nematic phase of sunset yellow, the simulations show chromonic columns with a loose hexagonal packing and an intercolumn distance of 2.36 nm. Partial condensation of sodium ions occurs around a chromonic stack, with two preferred binding sites identified for sodium ions, corresponding to strong binding with the oxygens of a sulfonate group and a bridging site between a pair of molecules in a stack. A value for the free energy of binding of a molecule to a stack of 7 k_BT was obtained for stacks of three and eight molecules, with a slightly larger value (additional 2 kJ mol^{-1}) obtained for the dimer binding energy, indicating that aggregation is approximately isodesmic.

Introduction

Chromonics are a fascinating class of lyotropic liquid crystals (LLC), which have recently become an active field of research.[1−4] Chromonic phases are usually formed in water from disk-like or plate-like molecules. Here, molecular self-assembly occurs into aggregates (stacks), with the stacks then able to pack to form liquid crystalline phases. Unlike many lyotropic liquid crystals, for chromonics self-assembly occurs at very low concentrations[1] and appears to be enthalpy driven rather than mediated by the hydrophobic effect (i.e., entropic interactions). Moreover, in chromonic systems the number of molecules in an aggregate tends to be unconstrained, and aggregation takes place at all concentrations (without a critical micelle concentration), with the distribution of aggregate sizes tending toward larger aggregates as the concentration increases. For many systems it is suggested that aggregation follows the isodesmic model.[5−8] Chromonic molecules are often chemically distinct from conventional lyotropic amphiphiles. They tend to have disk-like (rather than rod-like) shapes, possess a rigid core (rather than a flexible chain), and tend to be formed from aromatics rather than aliphatic moieties.

The first and most extensively studied chromonic LC was the anti-asthmatic drug disodium chromoglycate (Intal), which exhibits the two classic chromonic phases: N and M.[1,9−12] The name of this class of LC was adapted from the chromonyl group present in Intal, and in a range of other chromone derivatives, which exhibited optical textures characteristic of this type of mesogenic ordering.[1,13,14] More recently, formation of stacked aggregates in dilute solution and/or chromonic mesophases at higher concentrations have been widely reported in aqueous dispersions of many formulated products, such as pharmaceuticals and dyes used in inkjet printing. Recently, there has been enhanced interest in chromonics materials arising from potential uses as functional materials for fabricating highly ordered thin films[15,16] and as biosensors.[17,18] Chromonic stacks have also been used to aid in the controllable self-assembly of gold nanorods.[19] Here, anisotropic electrostatic interactions between the chromonic stacks and the nanorods aid in either side-by-

(1) Wu, L.; Lal, J.; Simon, K. A.; Burton, E. A.; Luk, Y. Y. *J. Am. Chem. Soc.* **2009**, *131*, 7430–7443.
(2) Tomasik, M. R.; Collings, P. J. *J. Phys. Chem. B* **2008**, *112*, 9883–9889.
(3) Tam-Chang, S. W.; Huang, L. M. *Chem. Commun.* **2008**, 1957–1967.
(4) Mohanty, S.; Chou, S. H.; Brostrom, M.; Aguilera, J. *Mol. Simul.* **2006**, *32*, 1179–1185.
(5) Henderson, J. R. *Phys. Rev. Lett.* **1996**, *77*, 2316–2319.
(6) Henderson, J. R. *Phys. Rev. E* **1997**, *55*, 5731–5742.
(7) Henderson, J. R. *J. Chem. Phys.* **2009**, *130*, 45101–45103.
(8) Smulders, M. M. J.; Nieuwenhuizen, M. M. L.; de Greef, T. F. A.; van der Schoot, P.; Schenning, A. P. H. J.; Meijer, E. W. *Chem.—Eur. J.* **2010**, *16*, 362–367.
(9) Lydon, J. E. *Mol. Cryst. Liq. Cryst.* **1980**, *64*, 19–24.
(10) Attwood, T. K.; Lydon, J. E. *Mol. Cryst. Liq. Cryst.* **1984**, *108*, 349–357.
(11) Nastishin, Y. A.; Liu, H.; Schneider, T.; Nazarenko, V.; Vasyuta, R.; Shiyanovskii, S. V.; Lavrentovich, O. D. *Phys. Rev. E* **2005**, *72*, 41711.
(12) Kostko, A. F.; Cipriano, B. H.; Pinchuk, O. A.; Ziserman, L.; Anisimov, M. A.; Danino, D.; Raghavan, S. R. *J. Phys. Chem. B* **2005**, *109*, 19126–19133.
(13) Lydon, J. *Curr. Opin. Colloid Interface Sci.* **2004**, *8*, 480–490.
(14) Simon, K. A.; Sejwal, P.; Gerecht, R. B.; Luk, Y. Y. *Langmuir* **2007**, *23*, 1453–1458.
(15) Kaznatcheev, K. V.; Dudin, P.; Lavrentovich, O. D.; Hitchcock, A. P. *Phys. Rev. E* **2007**, *76*, 61703.
(16) Olivier, Y.; Muccioli, L.; Lemaur, V.; Geerts, Y. H.; Zannoni, C.; Cornil, J. *J. Phys. Chem. B* **2009**, *113*, 14102–14111.
(17) Shiyanovskii, S. V.; Schneider, T.; Smalyukh, I. I.; Ishikawa, T.; Niehaus, G. D.; Doane, K. J.; Woolverton, C. J.; Lavrentovich, O. D. *Phys. Rev. E* **2005**, *71*, 20702.
(18) Shiyanovskii, S. V.; Lavrentovich, O. D.; Schneider, T.; Ishikawa, T.; Smalyukh, I. I.; Woolverton, C. J.; Niehaus, G. D.; Doane, K. J. *Mol. Cryst. Liq. Cryst.* **2005**, *434*, 587–598.
(19) Park, H. S.; Agarwal, A.; Kotov, N. A.; Lavrentovich, O. D. *Langmuir* **2008**, *24*, 13833–13837.

10.1021/ja102468g

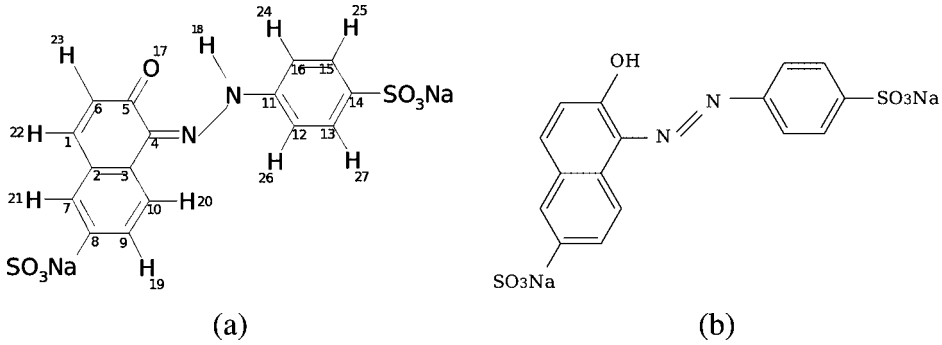

Figure 1. Molecular structure of SSY: (a) NH hydrazone form and (b) hydroxy azo form.

side or end-to-end assembly, depending on the surface charge of the nanorods.

The dianionic monoazo food dye edicol, sunset yellow (SSY), is a representative system for the many dye molecules known to aggregate in aqueous solution and form chromonic liquid crystals. The structure of the SSY molecule (shown in Figure 1) is typical of many chromonic materials. It contains central aromatic groups (phenyl and naphthyl rings linked via an azo group), with two solubilizing sulfonate groups attached to either end of the molecule. The UV−visible absorption spectrum shows a blue shift with increasing concentration of SSY in dilute aqueous solution,[20] implying that the molecules form H-aggregates (rather than J-aggregates) on association. At higher concentrations SSY shows two chromonic mesophases: a nematic (N) phase between 30 and 40 wt % and a hexagonal or middle phase (M) between 40 and 45 wt %.[20−23] X-ray diffraction (XRD) indicates that the aggregates found in mesophases are single-molecule stacks, with a typical stacking distance of 3.3−3.5 Å,[21−23] commensurate with the distance expected from the stacking of aromatic groups.

In this article we report the application of computational methods to explore the structure and dynamics of aggregates of sunset yellow in aqueous solution. Calculations are presented which, for the first time, show the details of molecular organization and dynamics of molecules within a chromonic stack, provide the binding free energy of a molecule to a short stack, and provide the first simulations of a bulk chromonic liquid crystal phase. Simulation results are compared to recent diffraction and spectroscopic data for SSY, allowing for a critical assessment of aggregation in these systems.

The paper is organized as follows. The next section contains details of the simulations carried out. The first section of the Results and Discussion provides structural and spectroscopic data from high-quality density functional theory calculations for SSY. The main results section reports bulk-phase simulations for a solvated SSY aggregate in dilute aqueous solution, providing detailed information about the structure and dynamics of a chromonic stack with comparisons to existing experimental data. The section also presents results from simulations in concentrated aqueous solution, corresponding to the bulk N phase of a chromonic liquid crystal. The final results section reports free energy calculations to investigate pairwise association energies and the binding of a molecule to small aggregate stacks in solution. Conclusions are drawn in the final section of the paper.

Computational Details

Quantum Chemical Calculations. The quantum chemical calculations used density functional theory (DFT), employing Becke's three-parameter hybrid exchange functional (B3)[24] combined with the correlation functional of Lee, Yang, and Parr (LYP),[25] together with a 6-311G** basis set for all atoms within the Gaussian 03 program.[26] Single-molecule calculations were fully optimized at this level of theory, and NMR chemical shieldings were subsequently calculated at the same level of theory using the GIAO method.[27] Calculations on molecular trimers used geometries obtained from molecular dynamics (MD) simulations. Some calculations employed an implicit solvation model for water provided by a polarizable continuum model (PCM).[28] Transitions energies and oscillator strengths were obtained for the first excited states of single molecules by use of the time-dependent DFT (TDDFT) method.[29,30]

Molecular Dynamics Simulation Model. The MD calculations employed the GAFF[31,32] force field parameters (Table S1, Supporting Information) in the AMBER force field,

$$E_{\text{total}} = \sum_{\text{bonds}} K_r(r - r_{\text{eq}})^2 + \sum_{\text{angles}} K_\theta(\theta - \theta_{\text{eq}})^2 + \sum_{\text{dihedrals}} \frac{V_n}{2}[1 + \cos(n\phi - \gamma)] + \sum_{i<j}\left[\frac{A_{ij}}{R_{ij}^{12}} - \frac{B_{ij}}{R_{ij}^{6}} + \frac{q_i q_j}{\varepsilon R_{ij}}\right] \quad (1)$$

where the parameters take their usual meaning.[31] The optimized structure of SSY, obtained from the DFT calculations, was used to provide an initial starting geometry, and atomic charges were obtained by fitting to the electrostatic potential around the molecule

(20) Horowitz, V. R.; Janowitz, L. A.; Modic, A. L.; Heiney, P. A.; Collings, P. J. *Phys. Rev. E* **2005**, *72*, 41710.
(21) Edwards, D. J.; Jones, J. W.; Lozman, O.; Ormerod, A. P.; Sintyureva, M.; Tiddy, G. J. T. *J. Phys. Chem. B* **2008**, *112*, 14628–14636. In this reference the assignments quoted for protons 19 and 20 (figure 1) were transposed in error. A correction has been provided by the authors. (Source: personal communication with Prof. G. J. T. Tiddy.).
(22) Joshi, L.; Kang, S. W.; Agra-Kooijman, D. M.; Kumar, S. *Phys. Rev. E* **2009**, *80*, 41703.
(23) Prasad, S. K.; Nair, G. G.; Hegde, G.; Jayalakshmi, V. *J. Phys. Chem. B* **2007**, *111*, 9741–9746.
(24) Becke, A. *J. Chem. Phys.* **1993**, *98*, 5648.
(25) Lee, C.; Yang, W.; Parr, R. G. *Phys. Rev.* **1988**, *37*, 785.
(26) Frisch, M. J.; et al. *Gaussian 03*, Revision C.02; Gaussian, Inc.: Wallingford, CT, 2004.
(27) Wolinski, K.; Hinton, J. F.; Pulay, P. *J. Am. Chem. Soc.* **1990**, *112*, 8251–8260.
(28) Tomasi, J.; Mennucci, B.; Cammi, R. *Chem. Rev.* **2005**, *105*, 2999–3093.
(29) Casida, M. E.; Jamorski, C.; Casida, K. C.; Salahub, D. R. *J. Chem. Phys.* **1998**, *108*, 4439–4449.
(30) Casida, M. E. *J. Mol. Struct.−Theochem* **2009**, *914*, 3–18.
(31) Wang, J. M.; Wolf, R. M.; Caldwell, J. W.; Kollman, P. A.; Case, D. A. *J. Comput. Chem.* **2004**, *25*, 1157–1174.
(32) Case, D. A.; Cheatham, T. E.; Darden, T.; Gohlke, H.; Luo, R.; Merz, K. M.; Onufriev, A.; Simmerling, C.; Wang, B.; Woods, R. J. *J. Comput. Chem.* **2005**, *26*, 1668–1688.

using the CHELPG scheme[33] in Gaussian 03. These force field parameters were used in the subsequent MD simulations described below.

For the MD work, two models of interest were identified, corresponding to dilute and concentrated SSY solutions. The model for SSY at a concentration of 5 wt % consisted of a preformed aggregate of eight dye molecules stacked in parallel at a distance of 3.5 Å. The stack was solvated with 3653 TIP3P[34] water molecules in a cubic box of dimensions $(53\ \text{Å})^3$. We also investigated the self-assembly of eight SSY molecules at the same concentration into a stack starting from a dispersed system of SSY monomers in the same solvent (see below). Here, to obtain an initial complete dispersion of dye molecules, we removed all Lennard-Jones interactions between the SSY atoms and equilibrated for 2 ns, prior to switching these interactions back on to begin the self-assembly production run. The model for SSY at a concentration of 33 wt % (which corresponded to a concentration where the nematic phase was expected) was built from 9 stacks of 16 molecules each, with stacks arranged initially on a square packaged lattice. For this calculation a total of 144 SSY dye molecules were solvated in 6424 TIP3P waters. The columns were rendered infinitely long by the periodic boundary conditions.

Initial MD simulations were carried out in the canonical (const-*NVT*) ensemble to equilibrate each system (typically equilibration runs were carried out for tens of nanoseconds), followed by production runs of typically 100−200 ns (see below for system-specific details) in the isobaric−isothermal (const-*NpT*) ensemble at a constant pressure of 1 atm. The MD simulations used the AMBER program with a MD time step of 1 fs throughout. The temperature of the system was maintained at 300 K using a Langevin thermostat with a friction coefficient of 1 ps^{-1}. The long-range part of the Coulomb potential was represented by employing an Ewald summation.

Results and Discussion

Molecular Structure of Sunset Yellow from Quantum Chemical Calculations. SSY has the potential to exist in either an NH hydrazone form (Figure 1a) or an OH hydroxy azo form (Figure 1b). This tautomerism is common in many azo dyes, and the proportion of each tautomeric structure present is influenced by whether a donating or withdrawing electron group is attached to C_{14} (Figure 1). We assessed the configurational energy of each form by initially carrying out DFT calculations for the hydrazone and hydroxy azo forms of SSY for the dianion and also for the neutral molecule with protonated (SO_3H) sulfonate groups. The DFT calculations pointed to the stability of the hydrazone form relative to the hydroxy azo structure for both the dianion and the protonated compound. For the dianion, the hydrazone structure is favored by 7.8 kJ mol^{-1}, which increases to 12.3 kJ mol^{-1} if the calculations are repeated with the implicit water solvation model. This suggests that almost 100% of this structure is likely to be present in aqueous solution, which is in good agreement with recent NMR measurements. Edwards et al.[21] quote a ^{13}C NMR chemical shift of ∼180 ppm for C_5 (Figure 1a), at both high and low concentrations of SSY in water, which is consistent with a C═O and not an aromatic C−OH (with expected chemical shift of ∼165 ppm). We therefore expect the NH tautomeric form to be present in SSY regardless of extent of aggregation.

Key bond lengths, angles, and dihedral angles from the optimized DFT structure are listed in Table S2 (Supporting Information). Most of the calculated bond lengths are comparable to those found in closely related dyes, which are known to be predominantly in the hydrazone form. This lowest energy conformation in SSY corresponds to a planar structure with the two aromatic groups in a trans configuration about the N−N bond. The $O_{17}\cdots H_{18}$ distance (1.7 Å) is significantly less than the sum of the van der Waals radii (2.6 Å), confirming the presence of an internal hydrogen bond. The lengthening of the N−N and C_4-C_5 distances in the hydrazone structure is accompanied by a complementary shortening of the $N-C_4$ and C_5-O_{17} bonds relative to the hydroxy azo form. The barrier to rotation about the N−N bond calculated from the DFT is ∼160 kJ mol^{-1}, indicating that SSY shows little conformational flexibility about this bond. The GAFF force field does a good job in reproducing the planar DFT structure and also the high DFT energy barrier to rotation about the N−N bond. However, the prediction of the trans−cis energy difference is rather poor. This is not important for this work, as the energy difference is so great (>60 kJ mol^{-1} in GAFF and higher still in the DFT calculations) that the population of the cis conformer is vanishingly small. The predicted barrier for rotation about the C−S bond is low (0.22 kJ/mol), meaning essentially free rotation is possible for this group.

Calculated transition energies, *E*, and oscillator strengths, *f*, for the first excited states determined by TDDFT are listed in Table 1. Experimentally, SSY shows a very intense visible absorption band at 480 nm in water,[20] which is reasonably well-predicted by a single-molecule calculation when solvent effects are accounted for.

The predicted ^{13}C and ^{1}H NMR chemical shifts are in good agreement with experiment. These are given in Table 2 relative to tetramethylsilane (TMS) resonances at the same level of theory, along with experimental values measured for SSY in D_2O solution.[21] The calculated ^{13}C resonances are generally within ca. 3 ppm of the experimental values, except for the

Table 1. Calculated Transition Energies (*E*), Wavelengths (λ), and Oscillator Strengths (*f*) for SSY in Different Environments, Together with Experimental UV−Visible Absorption Data[20]

gas phase			solvated			
E (eV)	λ (nm)	*f*	*E* (eV)	λ (nm)	*f*	expt λ (nm)
2.44	507.9	0.433	2.69	459.5	0.695	480
2.83	437.9	0.189	3.14	394.2	0.146	400
3.21	386.2	0.041	4.14	299.3	0.197	312

Table 2. Calculated and Experimental ^{13}C and ^{1}H NMR Shifts (δ, ppm)

	calcd				calcd		
atom[a]	gas	solv[b]	expt[21]	atom	gas	solv[b]	expt[21]
C_1	143.3	145.6	142.7	C_8	158.6	153.4	140.5
C_2	125.6	127.7	127.2	C_9	131.3	127.8	126.0
C_3	133.6	136.7	134.6	C_{10}	119.5	122.3	122.3
C_4	130.6	131.6	143.4	C_{11}	140.3	144.4	129.3
C_5	178.7	178.3	178.7	$C_{12,16}$	114.7	116.6	117.1
C_6	123.3	128.5	126.3	$C_{13,15}$	128.2	127.6	127.2
C_7	126	126.4	126.5	C_{14}	160.5	154.7	140.1
H_{19}[c]	7.613	8.433	8.383	H_{23}	6.048	6.814	6.610
H_{20}[c]	8.036	7.852	7.818	$H_{24,26}$	7.041	7.665	7.618
H_{21}	7.691	7.671	7.864	$H_{25,27}$	7.565	7.699	7.777
H_{22}	7.179	7.882	7.662				

[a] Figure 1a for SSY atoms assignment. [b] Polarizable continuum model (PCM) for water was used for the solvated phase. [c] The experimental results for protons 19 and 20 are corrected from a misassignment in the original paper.[21]

(33) Breneman, C. M.; Wiberg, K. B. *J. Comput. Chem.* **1990**, *11*, 361–373.
(34) Mark, P.; Nilsson, L. *J. Phys. Chem. A* **2001**, *105*, 9954–9960.

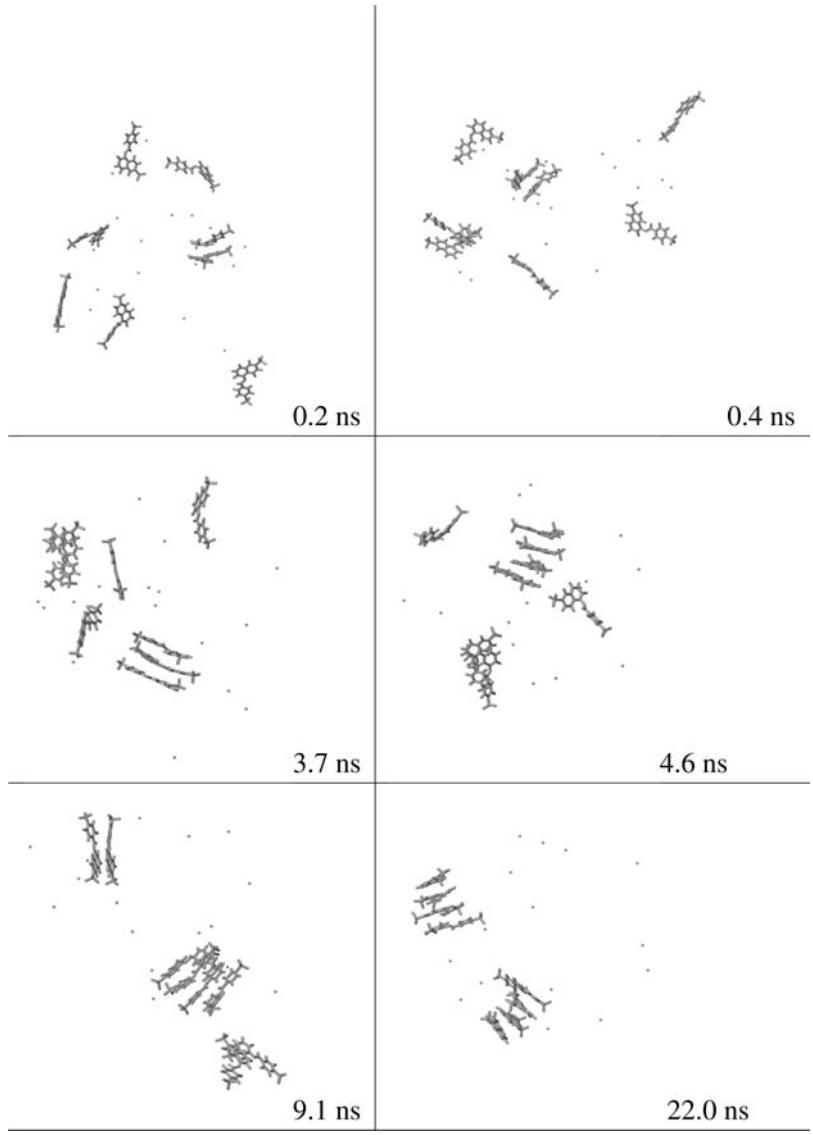

Figure 2. Snapshots showing the formation of dimer, trimer, and tetramer aggregates from an initial dispersion of isolated SSY molecules in aqueous solution.

carbon atoms within the azo link (C_4, C_{11}) and those near sulfonate groups (C_8, C_{14}), which are over ca. 10 ppm in error. The errors are likely attributable to insufficient treatment of electron correlation for the carbons in close proximity to the azo and sulfonate groups. It has been reported that MP2 calculations are often more accurate than DFT in predicting chemical shifts for carbons attached to N nuclei,[35] but the former are computationally expensive for large molecules such as SSY. For C_8 and C_{14} resonances, the difference may also arise from neglect of solvation effects for the nearby unprotonated sulfonate groups. Calculations for these nuclei in implicit water show improved agreement with experiment. The ^{13}C chemical shift for the C_5 resonance is characteristic of an NH tautomer (see above). The calculated ^1H resonances also compare well with experimental values, particularly when solvation is accounted for. The H_{18} is not observed in the proton spectra as it undergoes fast exchange with D_2O solvent, while the calculated H_{23} signal is farther downfield than a normal aromatic proton resonance as a result of weak hydrogen bonding of the adjacent oxygen atom.

Structure of Chromonic Stacks in Aqueous Solution. Molecular self-assembly into a chromonic stack occurs quite rapidly in solution. For relatively short columns this process takes place on time scales that (with recent increases in available computer time) are now becoming accessible to atomistic simulation. In our initial calculations, starting from a fully dispersed system of eight molecules, less than 1 ns of simulation time was sufficient to see initial formation of dimers in solution (Figure 2). The system evolved to form two tetramers within 22 ns and a single stack of eight molecules within 200 ns through eventual merger of the two tetrameric aggregates.

The self-assembly process is most easily seen by viewing pair distances between molecules, as shown in Figure 3. The two tetramers form at different points in the simulation, in each case by a stepwise addition of monomers. Within the simulation the rapid exhaustion of the reservoir of monomers leads to the final self-assembly of two tetramers being rather slow (limited

(35) Karadakov, P. B.; Morokuma, K. *Chem. Phys. Lett.* **2000**, *317*, 589–596.

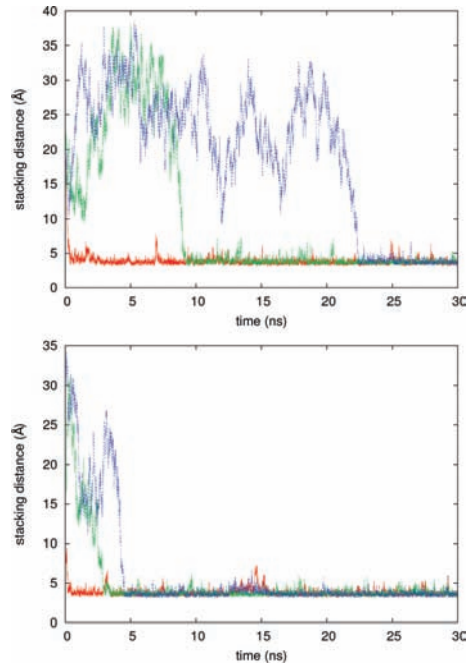

Figure 3. Time evolution of molecular distances between pairs of molecules during the formation of two SSY tetramers in aqueous solution. Red line, pair distances for molecules 1 and 2 within the final tetramer; green line, molecules 2 and 3; and blue line, molecules 3 and 4.

by tetramer diffusion). The latter, of course, would not occur in the thermodynamic limit. The binding between molecules is reasonably strong, and after self-assembly occurs the stack remains stable over hundreds of nanoseconds. This is consistent with a reasonably high binding energy for SSY molecules (as discussed in detail below).

Further simulations of a pre-assembled stack of eight molecules in solution reveal interesting structural and dynamical behavior over the course of a long 200 ns run. Visual inspection of the MD trajectories shows that the stack remains completely stable over the course of these long simulations but that molecules within the stack exhibit discrete rotational transitions superimposed on the slower translational and rotational diffusion time scale (1 ns) of the stack itself. The rotational transitions are infrequent but occur very rapidly within a short 10−100 ps time interval. A typical configuration from the stack simulation is shown in the side and plan view snapshots in Figure 4. The molecular stacking for SSY in Figure 4 has been inferred already from previous X-ray measurements of the N (nematic) and M (columnar) phases,[21,22,36] but previous assumptions of a circular cross-section seem questionable. Here, the molecules are seen to prefer an antiparallel configuration where the naphthyl ring is stacked on top of the phenyl ring and the C═O dipole alternates in direction along the stack. As shown by the plan view, this leads to a column with a preferred lath-like structure; i.e., the column cross-section is not circular, even in dilute solution. We note that the preference for antiparallel ordering has been seen in dielectric studies of dilute solutions of calamitic thermotropic mesogens with longitudinal dipoles.[37,38] In such systems, molecular association has been successfully described by a pairwise association model, which allows for both parallel and antiparallel dipole association.[37]

While the snapshots in Figure 4 show the preferred antiparallel stacking arrangement in the column, we stress that the organization in the column is dynamic. To assess this further we calculated the normalized orientational correlation function,

$$C_{ij}(t) = (\hat{r}_i \cdot \hat{r}_j) \qquad (2)$$

for the orientation of normalized bond vectors, $\hat{r}_i$, $\hat{r}_j$, representing the C═O dipole and the molecular axis (N−N vector) for adjacent pair of molecules i,j within the stack. Figure 5a−c shows the dipole−dipole correlation for three SSY pairs within the stack, for a simulation starting from an initial pre-assembled system with parallel C═O and N−N vectors. Memory of this initial arrangement is lost within ∼25 ns. Thereafter, the dipole correlation function shows rapid rotational "flips" occurring between a preferred antiparallel arrangement ($C_{ij}(t) \approx -1$) and a parallel dipole configuration with $C_{ij}(t) \approx 1$. These flips occur both rapidly and randomly, and a parallel configuration can remain for periods of over 10 ns. The preference for head-to-tail stacking is seen clearly in Figure 5d, which shows the correlation function for the molecular (N−N) axis for the two molecules in the center of the stack. The exact correspondence between this function and the C═O correlation function for the same molecules (Figure 5b) indicates that dipole flipping occurs by rotation about the short axis of the molecule parallel to the stacking direction, rather than by rotation around the long molecular axis. This is confirmed by MD trajectories following motion within

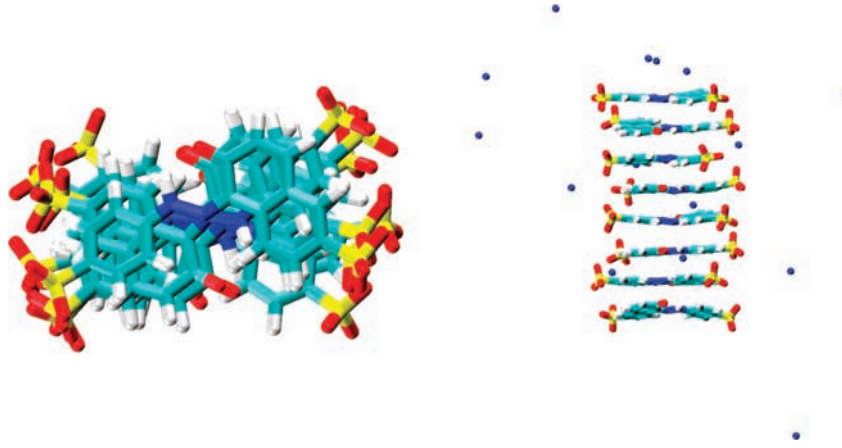

Figure 4. Snapshots showing the structure of an eight-molecule SSY aggregate in solution: left, view down the column, showing head-to-tail (antiparallel) stacking; right, view from the side of a column showing an alternation of the orientation of the C═O bond dipole and partial condensation of sodium ions.

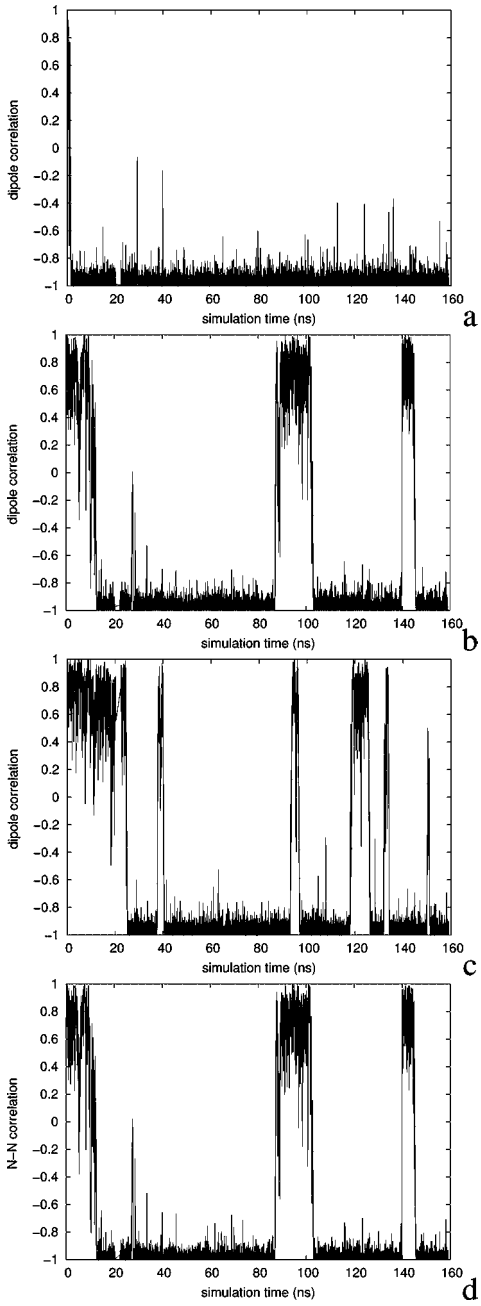

Figure 5. Time correlation function for normalized bond vectors starting from an initial parallel arrangement of molecules in a solvated stack: (a−c) C═O dipole−dipole correlation and (d) N−N azo−azo correlation.

the stack, which show that rotation about the short axis can occur without disruption to the structure of the stack itself.

Figure 6 shows the temporal evolution of the distance between two adjacent molecules. Here we show pair distances between SSY molecules at the base of the stack and distances of the molecular pair from the center of the stack. The stacking distance fluctuates around a mean value of 3.6 Å and is homogeneous along the stack. The distance shoot at 9 Å is due to either a twist or a shear of a molecular pair (see Supporting Information, Figure S1). The mean separation excluding stack rearrangement events is approximately 3.4 Å, which agrees closely with the experimental repeat distance seen in XRD measurements from the N phase.[21]

Previous authors[19,21,22] have noted the presence of four diffuse off-axis spots visible in the XRD of magnetically aligned N and M phases of SSY at ∼5.6 Å[19,22] or ∼6.8 Å,[21] which could be attributed to a nonplanar (oblique) orientation of the phenyl group with respect to the naphthalene plane, or from other effects such as formation of chiral arrangements of dye molecules within aggregates. Here, we note that the molecules appear perfectly planar within the aggregates, and we find (noting that we are able only to study relatively short columns) no evidence for chiral arrangements. However, we do find that head-to-tail packing leads to a chevron-type arrangement, as shown in Figure 4a, which may explain the presence of the four diffuse spots.

NMR studies have also been used to attempt to assess the nature of stacking within SSY aggregates. The ^{1}H resonances of SSY and other azo dyes have been reported to change by $\Delta\delta \approx 0.5-1.5$ ppm with increasing concentration in aqueous solution.[21,39] This is due to the intermolecular influence of aromatic ring-currents on shielding/deshielding, occurring as a result of molecular stacking.[40] To provide a crude estimate of the chemical shift changes on aggregation, the ^{1}H resonances for dimers and trimers were calculated using the same DFT functional and GIAO methodology used above, averaging over 20 dimer and 10 trimer configurations. In agreement with experiment, we find an increase in shielding for all protons on aggregation for both dimers and trimers, corresponding to a decrease in proton chemical shifts. In particular, findings of large shifts in trimer averages of ≥0.6 ppm for some protons at both ends of the molecule (H_{19}, 0.6 ± 0.2 ppm; H_{23}, 0.6 ± 0.2 ppm; $H_{24,26}$, 1.0 ± 0.2 ppm) are consistent with both the phenyl and naphthyl rings being involved in π-stacking, as seen in the snapshots of Figure 4 and as concluded by Edwards et al.[21]

Structure of the N-Phase. The time evolution of the concentrated SSY solution was followed over a period of 60 ns. During this time nematic columns form a pseudohexagonal packing arrangement. Interestingly, there is no direct contact between columns in the nematic phase; instead, the charged columns repel each other to form a loosely connected structure, where the columns are well-solvated with a dynamic structure very similar to that seen in the isolated columns. The preferred head-to-tail stacking of molecules (discussed above) also occurs within the nematic phase (side view in Figure 7). The intercolumn distance, calculated from the Fourier transform of the structure factor, $S(k)$, is 2.3 nm. This is in good agreement with XRD reflections from the nematic phase of SSY, which indicate interaggregate distances in the range of 20−30 Å depending on concentration.[20−23,41]

The radial distribution, $g(r)$, of Na^+ counterions with respect to SO_3^- groups is shown in Figure 8 for the nematic phase. The behavior of $g(r)$ remains qualitatively similar in both dilute and concentrated SSY solutions. Evidence for a partial condensation of sodium ions around the stack was seen in the earlier snapshots (Figure 4), and this is confirmed by the $g(r)$ results. A preferred "binding site" corresponding to a distance of 2.4 Å from a sulfonate oxygen (3.7 Å from a sulfonate sulfur) is evident in Figure 8, and a secondary site can be identified at a

(36) Dickinson, A. J.; LaRacuente, N. D.; McKitterick, C. B.; Collings, P. J. *Mol. Cryst. Liq. Cryst.* **2009**, *509*, 751–762.
(37) Toriyama, K.; Dunmur, D. A. *Mol. Cryst. Liq. Cryst.* **1986**, *139*, 123–142.
(38) Dunmur, D. A.; Toriyama, K. *Liq. Cryst.* **1986**, *1*, 169.
(39) Abbott, L. C.; Batchelor, S. N.; Oakes, J.; Smith, J. R. L.; Moore, J. N. *J. Phys. Chem. B* **2004**, *108*, 13726–13735.
(40) Adams, H.; Hunter, C. A.; Lawson, K. R.; Perkins, J.; Spey, S. E.; Urch, C. J.; Sanderson, J. M. *Chem.—Eur. J.* **2001**, *7*, 4863–4878.
(41) Park, H. S.; Kang, S. W.; Tortora, L.; Nastishin, Y.; Finotello, D.; Kumar, S.; Lavrentovich, O. D. *J. Phys. Chem. B* **2008**, *112*, 16307–16319.

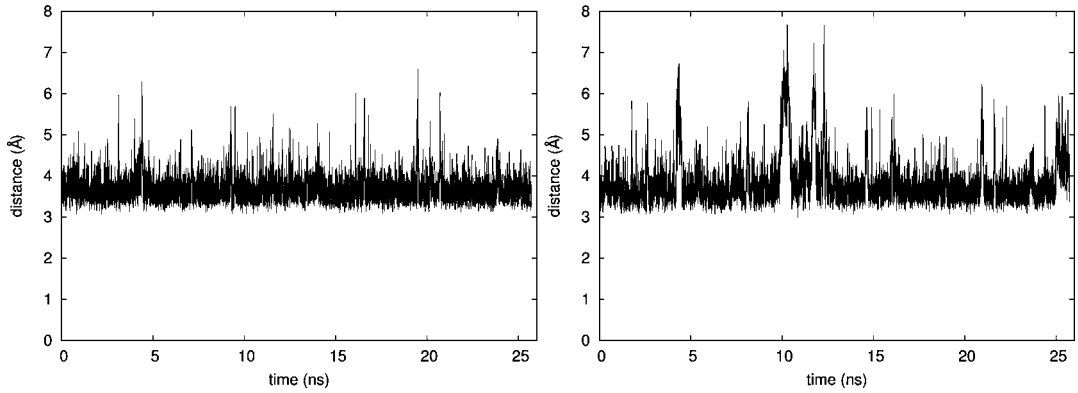

Figure 6. Stacking distance between pairs of SSY molecules (a) at the base of a stack and (b) in the center of a stack of eight molecules in aqueous solution.

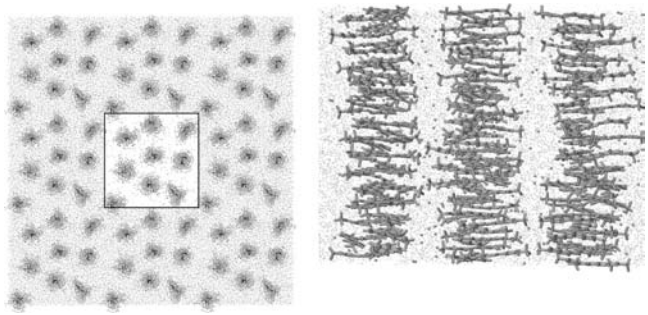

Figure 7. Plan and side view snapshots of the N phase taken from a 60 ns MD run. Plan view shows the periodic box surrounded by image boxes to illustrate the loose hexagonal packing of columns.

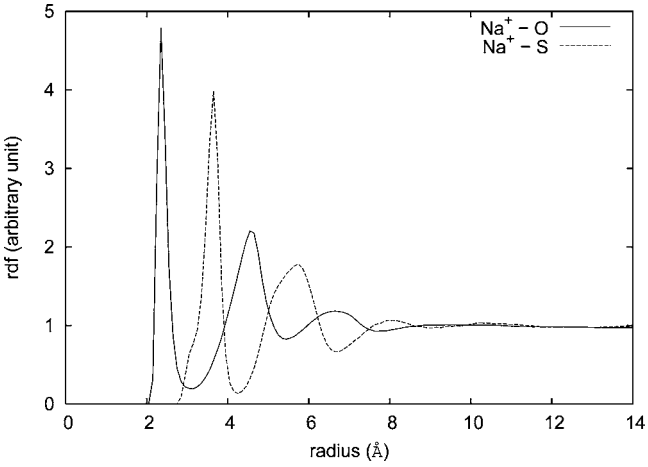

Figure 8. Radial distribution functions between sodium ions and oxygens of sulfonate groups and sulfurs in 33% SSY solution.

Na^+-O distance of 4.5 Å. The main peak corresponds to a favorable interaction with the three oxygens of a single sulfonate group. This binding site has a relatively long residence time. The second peak in $g(r)$ corresponds to an arrangement where sodium ions are able to bridge between two separate SSY molecules, forming a loosely held bridge. Hence, counterions never penetrate the stack but interact reasonably strongly with the surface charged groups. Setting 7.7 Å as a cutoff criterion for ions "bound" to the stack allows the fraction of "bound" and "free" ions to be calculated.

From the $g(r)$ graphs we estimate that the fraction of bound ions is 0.38 for the stack of 8 SSY molecules in dilute solution, rising to 0.44 for the stacks of 16 SSY molecules in a concentrated solution; i.e., on average approximately 7 Na^+ and 14 Na^+ are condensed on a stack of 8 and 16 molecules length, respectively (out of the 16 and 32 Na^+ needed to neutralize the charged stacks). Stacking of the SSY molecules creates a charged polyion with a charge of $2e^-$ per 3.4 Å, and a linear charge density $\nu = 2/(3.4\ \text{Å}) = 0.59\ \text{Å}^{-1}$. According to Manning theory,[42,43] counterion condensation onto the polyion occurs when the polyion charge density exceeds a critical value. For a rod-like polyion, such as a stack, the critical charge density ν_o is $\nu_o = (z\lambda_B)^{-1} = 0.14\ \text{Å}^{-1}$, where z is the counterion valence (i.e., +1 for sodium) and the Bjerrum length is given by $\lambda_B = e^2/(4\pi\varepsilon kT) = 7$ Å (with dielectric constant ε, elementary charge e, and thermal energy kT) for water solutions at 298 K. For our system ν is much higher than ν_o; thus, counterion condensation should take place to decrease the bare charge of the stack in agreement with simulation results.

Experimental evidence for ion binding can be provided from NMR quadrupole splittings of ^{23}Na ions, which are proportional to the fraction of bound species ξ. For anionic surfactant hexagonal phases, the splitting $\Delta^{23}Na$ is usually ca. 9−10 kHz, while for SSY it is 3−4 kHz,[21,44] corresponding to approximately 50% of bound sodium ions. Recent atomistic simulations[45] have considered the degree of counterion condensation for spherical surfactant micelles, e.g., cationic DTAC (65%) or anionic SDS (67%), and coarse-grained simulations for micelles have reported values in the range 50−80%.[46] Zhao et al.[47] showed, from an extensive MD study of an anionic POPG lipid bilayer, that about 60% of Na^+ ions are involved in interlipid interaction via ion bridge binding. For SSY the slightly smaller figure for bound ions can be explained by the rather irregular nature of the charged surface of the columnar aggregate compared to a micelle or a bilayer. By following individual Na^+ ions through the simulation, the average residence time for the strong binding interaction can be estimated as 33 ps. The constant orientational fluctuations in the stack also shorten the residence time for bridging ions. For our simulations, the fact that ξ is not strongly dependent on water

(42) Manning, G. S. *Macromolecules* **2007**, *40*, 8071–8081.
(43) Manning, G. S. *J. Phys. Chem. B* **2007**, *111*, 8554–8559.
(44) Wennerstrom, H.; Lindman, B.; Lindblom, G.; Tiddy, G. J. T. *J. Chem. Soc., Faraday Trans. 1* **1979**, *75*, 663–668.
(45) Jusufi, A.; Hynninen, A. P.; Haataja, M.; Panagiotopoulos, A. Z. *J. Phys. Chem. B* **2009**, *113*, 6314–6320.
(46) Bruce, C. D.; Berkowitz, M. L.; Perera, L.; Forbes, M. D. E. *J. Phys. Chem. B* **2002**, *106*, 3788–3793.
(47) Zhao, W.; Rog, T.; Gurtovenko, A. A.; Vattulainen, I.; Karttunen, M. *Biophys. J.* **2007**, *92*, 1114–1124.

content is indicative of the structure of the columns remaining quite similar in dilute solution and in the N phase.

Self-diffusion coefficients, D, can also be estimated for both water and sodium counterions. Here, D values were determined from the mean square displacement, $|r(t) - r(0)|^2$, using the Einstein relation,

$$D = \lim_{t\to\infty} \frac{1}{6t}\langle |r(t) - r(0)|^2 \rangle \quad (3)$$

Values of $D_{water} = 3 \times 10^{-9}$ and 1.2×10^{-9} m^2 s^{-1}, and $D_{Na} = 2.6 \times 10^{-9}$ and 0.4×10^{-9} m^2 s^{-1}, were obtained for 5% and 33% SSY, respectively. The reduction of the water self-diffusion coefficient is expected in the N phase because all water molecules have at least long-range interactions with a column at this concentration. This essentially eliminates completely free bulk water within this phase. The slow-down in dynamics within the nematic phase is also seen in reorientational motion. The mean decay of the time correlation function of the N−N bond vector is ∼0.33 ns in the dilute system and ∼1 ns in the N phase. This change arises from a reduction in the flipping rate of individual molecules within the N phase.

Free Energy of Binding to Aggregate Stacks. We adopted a nonequilibrium approach to calculate the free energy of binding based on the Jarzynski equality,[48,49]

$$e^{-\beta\Delta F} = \langle e^{-\beta W_{AB}} \rangle_A \quad (4)$$

where $\beta = (k_B T)^{-1}$, ΔF is the free energy difference between two equilibrium states A and B, W_{AB} is the nonequilibrium work performed on a system when going from state A to state B along a "reaction" coordinate, and the angular brackets denote the average over a canonical ensemble of the initial state A. We note that this approach has recently proved to be successful for systems undergoing large structural changes, e.g., excess chemical potentials for additive molecules in polymers,[50] ligand binding to proteins,[51] and structural transitions in peptides.[52−54]

To compute ΔF for pulling one molecule from a stack, the reaction coordinate, $\lambda(r)$, which in this case represents the distance separating the centers of mass of the molecule and the aggregate, was confined to a time-dependent harmonic potential,

$$U(r) = \frac{1}{2}k(\lambda(r) - \lambda_0 - \upsilon t) \quad (5)$$

where $\lambda(r)$ represents a chosen reaction path with an initial value λ_0 and υ is the pulling speed of the spring of force constant k. One molecule from the stack base was connected to a spring moving at a constant velocity 7 Å ns^{-1} with a force constant of 5000 kJ mol^{-1}. The simulation was discontinued when the spring had traveled a total distance of 1.2 nm. Several spring speeds were tried (see Supporting Information, Figure S2, for details), and we found that the larger velocities produced results comparable to those found for the slower velocities, providing that enough simulations were taken to produce meaningful

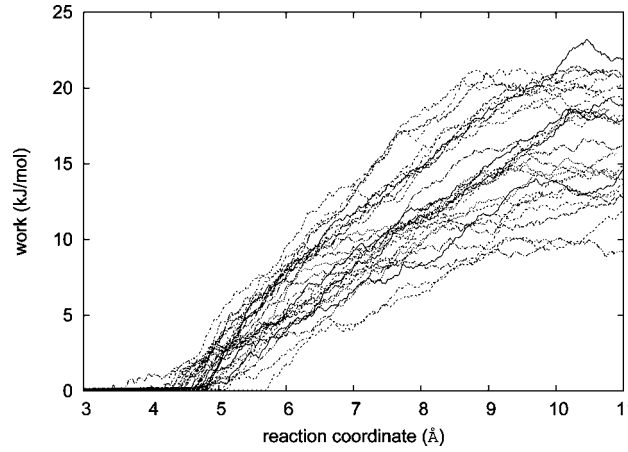

Figure 9. Profile of the work done in pulling one SSY molecule from a stack of eight molecules as a function of the distance separating their center of mass. A subset of 20 realizations is shown.

canonical averages. A set of steered molecular dynamics (SMD) simulations were carried out over an ensemble of starting configurations taken at equal time intervals from a previous 200 ns MD run of the eight SSY molecule stack. To assess the effect of the aggregate size on the binding, we also performed SMD runs for a SSY dimer and trimer in dilute solution. For these runs the starting configurations were taken from equilibrium MD runs for the dimer and the trimer at the same simulation conditions as the stack. Over 130 realizations were carried out for each case using the same pulling conditions.

Figure 9 shows the profile of the cumulative work required to pull a molecule from a stack. From the curve shown, the work increases steadily due to the strong attraction between the SSY molecule and the stack. At intermediate separations, water molecules form solvation shells between the two new interfaces of the pulled molecule and its nearest neighbor, so that at larger separations the work levels off. All realizations converged to a final state consisting of a single molecule and an aggregate of size $(n - 1)$ (where n is the number of SSY molecules in the initial aggregate). A histogram of work values is plotted in Figure 10 for each aggregate. The distribution of the work values is approximately gaussian, and low values corresponding to low-energy paths are reasonably well-sampled. Hence, the sampling provides confidence that enough realizations have been made to provide good estimates for ΔF.[50] The free energy change in Table 3 is estimated from the exponential average (eq 4), and we give also the second-order cumulant $\langle W \rangle - \beta\sigma^2/2$ (noting that this value is always, as expected, below the ordinary average of the work). The uncertainty in ΔF was estimated using the bootstrap method.[55] In this method, N work values were chosen at random (with replacement) from the distribution, and the free energy was evaluated from the exponential average of these values. This procedure was repeated 10^5 times, and the error is then given by the standard error of the resulting free energies. The binding free energy for a molecule in an aggregate is estimated to be approximately 7 $k_B T$ (16.3 kJ mol^{-1}).[20] This is in very close agreement with experimental values of 7.25 ± 0.01 $k_B T$ reported by Horowitz et al.[20] from UV−vis spectra and 7.4 $k_B T$ estimated by Park et al.[41] from changes in the line width of X-ray peaks. For a closely related dye, Bordeau dye, ΔF was found to be 9.2 ± 0.4 $k_B T$ from UV−vis spectra[2] and 10 $k_B T$ from X-ray analysis.[36] Since Bordeau dye forms aggregates at lower concentration than

(48) Jarzynski, C. *Phys. Rev. E* **1997**, *56*, 5018–5035.
(49) Jarzynski, C. *Phys. Rev. Lett.* **1997**, *78*, 2690–2693.
(50) Hess, B.; Peter, C.; Ozal, T.; van der Vegt, N. F. A. *Macromolecules* **2008**, *41*, 2283–2289.
(51) Ytreberg, F. M. *Biol. Phys.* **2008**, *978*, 65–74.
(52) Xiong, H.; Crespo, A.; Marti, M.; Estrin, D.; Roitberg, A. E. *Theor. Chem. Acc.* **2006**, *116*, 338–346.
(53) Crespo, A.; Marti, M. A.; Estrin, D. A.; Roitberg, A. E. *J. Am. Chem. Soc.* **2005**, *127*, 6940–6941.
(54) Park, S.; Khalili-Araghi, F.; Tajkhorshid, E.; Schulten, K. *J. Chem. Phys.* **2003**, *119*, 3559–3566.
(55) Efron, B.; Tibshirani, R. *Stat. Sci.* **1986**, *1*, 54.

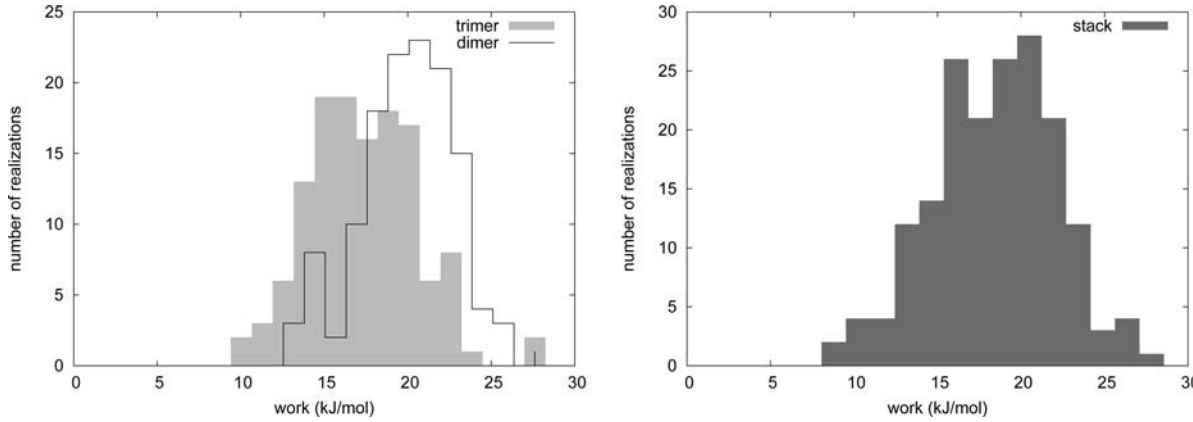

Figure 10. Histogram showing the distribution of work values obtained for the removal of one SSY molecule from aggregates of different sizes: left, removal of a SSY molecule from a dimer and a trimer; right, removal of a SSY molecule from a stack of eight molecules.

Table 3. Results (in kJ/mol) from *N* Pulling Realizations[a]

SSY aggregate	*N*	$\langle W \rangle$	$\sigma(W)$	$\langle W \rangle - 0.5\beta\sigma^2$	ΔF	eed
dimer	130	20.03	2.85	18.41	18.33	3.59
trimer	130	17.99	3.24	15.89	16.12	2.64
stack	178	19.12	3.73	16.33	16.30	2.41

[a] $\langle W \rangle$ is the average work value, with standard deviation $\sigma(W)$. ΔF is the free energy estimated from the second cumulant by assuming the work distribution is gaussian (column 5) and from Jarzynski's equality eq 4 (column 6). eed is the uncertainty estimate in ΔF calculated via a bootstrap method.

SSY and forms liquid crystals at considerably lower concentrations, the ΔF values seem to be in line with expectations. We note that Joshi et al.[22] have used X-ray analysis to report values for ΔF in the nematic phase, which are lower ($4.3 \pm 0.3\ k_BT$) than those measured in dilute solution.

The UV−vis measurements of Horowitz et al.[20] and Tomasik and Collings[2] were obtained from fitting absorption data, under the assumption that the isodesmic theory of aggregation works for these systems.[2,20] In our free energy calculations, within the error bars obtained, we predict no difference in the binding energy for a monomer on moving from a trimer to an octamer stack. However, from the final mean values and from the free energy histograms, there is clear indication that the free energy change is slightly higher for the dimer by a small amount ($\sim$2 kJ mol^{-1}). Hence, aggregation is approximately isodesmic[56] but shows a small deviation for a dimer, as suggested by Henderson.[7] It could therefore be well-modeled by a two-equilibrium-constant model.[7,8] It should be noted that, for this strength of aggregation, it would be very difficult to simulate the exponential aggregate distribution (expected from isodesmic chemical equilibria) at an atomistic level. Here, periodic boundary conditions and a small reservoir of molecules are predicted to dramatically favor large clusters, as shown recently by Henderson.[57] For our model, many thousands of SSY molecules may be required to obtain a cluster distribution close to that expected in the thermodynamic limit.

An interesting fundamental question arises as to whether the strong aggregation seen here can be attributed to strong attraction between the disks themselves, or from the solvent molecules hating the central aromatic regions of the disk-shaped solute.[58] One possible way of testing this would be to grow a solute molecule (with associated ions and solvent around the rim of the disk) into the solvent and measure the free energy change for this process. However, the errors associated with such a calculation (either via a none-equilibrium Jarzynski approach or by other free energy methods) would be very difficult to control for a solute as large as SSY, making this a very computationally challenging problem.

Conclusions

We have carried out the first detailed atomic simulation study of molecular order within a chromonic liquid crystalline material (SSY) in aqueous solution. The results show formation of a stable chromonic aggregate of molecules with a preference for head-to-tail stacking. This feature is independent of the concentration of the solution and aggregate size. At a concentration matching the nematic phase of SSY, the simulations show chromonic columns with a loose hexagonal packing and an intercolumn distance of 2.36 nm. Two preferred binding sites were identified for sodium ions, corresponding to strong binding with the oxygens of a single SO_3^- group and a bridging site between a pair of molecules in a stack. The number of condensed sodium ions changes by only a small amount on going from dilute to concentrated solution, and over half the sodium ions can be classified as unbound. Aggregation in dilute solution is approximately isodesmic. The computed free energy of binding is the same for stacks of three and eight molecules but is slightly larger for a dimer, and so it could suitably be modeled by a two-equilibrium-constant model.

Acknowledgment. We thank EPSRC for financial support. Thanks to Dr. J. W. Jones and Prof. G. J. T. Tiddy (University of Manchester) for numerous discussions and for providing experimental data and preprints of their recent manuscripts. We are also grateful for very helpful discussions and support from Prof. A. J. Masters (University of Manchester), Dr. J. Lydon (University of Leeds), and Dr. O. Lozman (Fujifilm).

Supporting Information Available: Complete ref 26, GAFF force field parameters for SSY, selected optimized structural parameters for SSY hydrazone form, snapshots of a chromonic stack showing molecular reorientation and slip in the center of the stack, and work profiles to remove a monomer from the end of a chromonic stack. This material is available free of charge via the Internet at http://pubs.acs.org.

JA102468G

(56) Maiti, P. K.; Lansac, Y.; Glaser, M. A.; Clark, N. A. *Liq. Cryst.* **2002**, *29*, 619–626.
(57) Henderson, J. R. *Phys. Rev. E* **2008**, *77*, 030401.
(58) Henderson, J. R. *J. Chem. Phys.* **2000**, *113*, 5965–5970.